

# Separation of $\text{Cu}^{2+}$ and $\text{Pb}^{2+}$ by tetraethylenepentamine-modified sugarcane bagasse fixed-bed column: selective adsorption and kinetics

J. Yu<sup>1</sup> · W. Xiong<sup>1</sup> · J. Zhu<sup>1</sup> · R. Chi<sup>1</sup>

Received: 3 March 2016/Revised: 19 April 2016/Accepted: 3 May 2016/Published online: 23 May 2016  
© Islamic Azad University (IAU) 2016

**Abstract** Tetraethylenepentamine-modified sugarcane bagasse (SCB) was prepared to improve its adsorption capacity and selectivity toward  $\text{Cu}^{2+}$ . Adsorption performances of the modified sorbent for  $\text{Cu}^{2+}$  were studied in batch system. Separation of  $\text{Cu}^{2+}$  from  $\text{Pb}^{2+}$  by the modified sorbent fixed-bed column were studied under dynamic system with initial molar concentration ratio ( $C_0^{\text{Cu}}/C_0^{\text{Pb}}$ ) ranging from 1:1 to 1:100. The amount of  $\text{Cu}^{2+}$  and  $\text{Pb}^{2+}$  adsorbed on the saturated column was calculated by the elution curve. Batch experimental results showed that the adsorption capacity of the sorbent for  $\text{Cu}^{2+}$  increased from 0.12 to 0.21  $\text{mmol g}^{-1}$  after modification. Dynamic adsorption results showed that the modified SCB had higher adsorption affinity toward  $\text{Cu}^{2+}$  than  $\text{Pb}^{2+}$ . 0.07  $\text{mmol g}^{-1}$  of adsorbed  $\text{Pb}^{2+}$  was pushed off by  $\text{Cu}^{2+}$  during the competitive adsorption process at  $C_0^{\text{Cu}}/C_0^{\text{Pb}} = 1:1$ . The breakthrough curves and adsorption kinetics of  $\text{Cu}^{2+}$  in the column could be fitted well by the Yoon–Nelson and modified Yoon–Nelson model, respectively. According to the elution curve, the amount of  $\text{Cu}^{2+}$  adsorbed on the fixed-bed column were 0.16, 0.16 and 0.15  $\text{mmol g}^{-1}$ , while that of  $\text{Pb}^{2+}$  were 0.0016, 0.0051 and 0.0094  $\text{mmol g}^{-1}$  when  $C_0^{\text{Cu}}/C_0^{\text{Pb}}$  increased from 1:1 to 1:10 and 1:100.  $\text{Cu}^{2+}$  could be selectively adsorbed and separated from  $\text{Pb}^{2+}$  by using the modified sorbent fixed-bed column.

**Keywords** Amination · Sugarcane bagasse · Dynamic adsorption ·  $\text{Cu}^{2+}$  ·  $\text{Pb}^{2+}$

## Introduction

With the development of society, large amounts of wastewater containing heavy metals, especially  $\text{Cu}^{2+}$  and  $\text{Pb}^{2+}$ , are produced (Qaiser et al. 2009).  $\text{Cu}^{2+}$  and  $\text{Pb}^{2+}$  are non-biodegradable and tends accumulate in organisms as part of the food chain (Motsa et al., 2011; Deng et al., 2013), which would cause severe damage to ecosystem (Naiya et al. 2009; Xu et al. 2008). Treatment of this wastewater becomes a worldwide problem. A variety of methods, including chemical precipitation, membrane processes, coagulation, adsorption and biosorption had been reported to remove heavy metals from aqueous solution (Isaac et al. 1997). Among these methods, biosorption is recognized as an efficient and economic method. Agricultural wastes such as sugarcane bagasse, rice husk and coir pith were used to remove metal ions from aqueous solution (Nguyen et al. 2013; Krishnan et al. 2011; Nembr et al. 2015; Krishnan et al. 2016). However, the unmodified agricultural waste had poor adsorption capacity and selectivity toward heavy metals. Currently, more attention is paid to the preparation of functional groups-modified sorbent with high adsorption capacity (Madrid et al. 2014; Hu et al. 2011; Xu et al. 2013; Goyal and Srivastava 2009). Little work is focused on the utilization of the modified sorbent to separate and recycle of metal ions with similar properties such as  $\text{Cu}^{2+}$  and  $\text{Pb}^{2+}$  from the aqueous solution.

It had been reported that different modified biosorbents had different adsorption affinity toward metal ions. Bayo (2012) had prepared modified grapefruit biomass and found

✉ R. Chi  
rac\_wit@163.com

<sup>1</sup> Key Laboratory for Green Chemical Process of Ministry of Education, Hubei Novel Reactor and Green Chemical Technology Key Laboratory, School of Chemistry and Environmental Engineering, Wuhan Institute of Technology, Wuhan 430074, China

that the adsorption affinity of this sorbent followed the order: Pb(II) > Cu(II) > Ni(II) > Cd(II). Yu et al. (2015a) reported that the adsorption affinity of sugarcane bagasse modified by carboxyl groups had the order: Pb(II) > Cu(II) > Cd(II) > Zn(II). Simate and Ndlovu (2015) found that the affinity order of immobilized cassava peel was:  $V^{3+} > Cr^{3+} > Co^{2+}$ . Rosales et al. (2015) reported that the binding affinity for the studied metals decreased in the following order: Cu(II) > Cr(VI) > Ni(II) > Zn(II) > Mn(II) for fern and oak leaves. Although the difference in adsorption affinity could not make the metal ions selectively adsorbed in a batch adsorption process, it provided a possibility to separate and recycle individual metals in dynamic system. Under this system, substitution reaction on the biosorbent occurred, and metal ions with high adsorption affinity would replace the one with lower adsorption affinity (Escudero et al. 2013; Nuic' et al. 2013). If the adsorption affinity difference between the metal ions was large enough, metal ions could be selectively adsorbed and separated. However, to our knowledge, separation of metal ions, especially  $Cu^{2+}$ , from other metal ions by the modified sorbent fixed-bed column had rarely been reported.

In this study, tetraethylenepentamine-modified sugarcane bagasse (SCB) was prepared by a simple method. Adsorption performances including isotherm and pH experiment of the modified SCB for  $Cu^{2+}$  were carried out in batch system. The effect of  $Pb^{2+}$  on the adsorption of  $Cu^{2+}$  was studied at different  $C_0^{Cu}/C_0^{Pb}$  under the dynamic system. The behavior and mechanism of selective adsorption and separation of  $Cu^{2+}$  from  $Pb^{2+}$  were discussed. The amount of  $Cu^{2+}$  and  $Pb^{2+}$  adsorbed on the modified SCB fixed-bed column was calculated through the elution curves by using ethylenediaminetetraacetic acid disodium salt as the eluent. The separation efficiency of the modified SCB fixed-bed column for  $Cu^{2+}$  and  $Pb^{2+}$  was determined.

## Materials and methods

### Materials

Sugarcane bagasse (SCB) was collected and bled white by the extractor, and then boiled in water for 1 h. Then it was washed with distilled water five times and dried at 60 °C for 24 h. The obtained SCB was grinded and sieved by 100 mesh before use. Tetraethylenepentamine (TEPA), epichlorohydrin, copper nitrate, lead nitrate and ethylenediaminetetraacetic acid disodium salt (EDTA-2Na) were purchased from Sinopharm Chemical Reagent Co., Ltd (Shanghai, China). Solutions of  $Cu^{2+}$  and  $Pb^{2+}$  were prepared using the corresponding metal nitrate.

### Surface modification

Amine groups-modified SCB was prepared by two a step method according to Yu et al. (2015b). First, during the cross-linking step, 120 mL of epichlorohydrin was added into 220 mL of NaOH solution ( $1.25 \text{ mol L}^{-1}$ ) containing 10.0 g of SCB. After reaction for 30 min at 40 °C, the sorbent was collected and washed with ethanol and distilled water. Second, during the amination step the cross-linked sorbent was added to 100 mL  $Na_2CO_3$  solution ( $0.1 \text{ mol L}^{-1}$ ) containing 10 mL of tetraethylenepentamine, and continued to react at 65 °C for 2 h under nitrogen atmosphere. The obtained sorbent was washed and dried in a vacuum oven at 60 °C for 24 h before use.

### Batch adsorption experiment

Adsorption performances including isotherm and pH experiment were carried out at room temperature and 150 rpm on an orbital shaker for 60 min. In the adsorption isotherms, 0.005 g of the modified or unmodified SCB was added into a 20 mL of  $Cu^{2+}$  solution with initial concentration ranging from 3 to 70  $\text{mg L}^{-1}$  at natural solution pH (pH 5.0). In the pH experiment, 0.005 g of the modified SCB was added into 20 mL of  $Cu^{2+}$  solution with initial concentration of 38.4  $\text{mg L}^{-1}$ . The residual concentration of  $Cu^{2+}$  after adsorption was determined by an atomic absorption spectrophotometer (AA6300, Shimadzu, Japan). All experiments were carried out in triplicate, and the reported values were average values of three data sets.

### Fixed-bed column adsorption experiment

The column experiments were conducted in a glass column with an inner diameter of 1 cm and height of 20 cm at room temperature. 0.5 g of the modified SCB was soaked in 100 mL of distilled water and then poured slowly into the column. After the adsorbent had settled, the column was pumped with distilled water for 30 min. Then, a solution of  $Cu^{2+}$  or mixture of  $Pb^{2+}$  and  $Cu^{2+}$  with mole ratio of 1:1, 10:1 and 100:1 were pumped into the fixed-bed column. Concentration of  $Cu^{2+}$  used in this experiment was fixed at 20  $\text{mg L}^{-1}$ . pH of the metal solution was kept at 4.0 for all adsorption experiment. For the column was initially filled with water, a control experiment using no SCB fixed in the column was performed at the same initial concentration of  $Cu^{2+}$  and  $Pb^{2+}$  in the unitary system to unequivocal data analysis concerning metal uptake in open system. Samples were collected at the exit of the column at different time intervals and analyzed for metal ion concentrations using an atomic absorption spectrophotometer. The amount of metal ions adsorbed on the fixed-bed column at time  $t$  ( $q_t$ ,  $\text{mmol g}^{-1}$ ) was calculated by the

following equation (integrated by using the software origin 8.0):

$$q_t = v \frac{\int_{t=0}^{t=t} (C_0 - C_t) dt}{m} \quad (1)$$

where  $v$  ( $\text{mL min}^{-1}$ ) is the volumetric flow rate.  $C_t$  ( $\text{mg L}^{-1}$ ) is the concentration of metal ion in the effluent at time  $t$ .  $C_0$  ( $\text{mg L}^{-1}$ ) is the inlet concentration of metal ion, and  $m$  is the mass of the modified SCB used in the fixed-bed column. All experiments were carried out in triplicates, and the reported values were average values of three data sets.

### Fixed-bed column desorption experiment

After exhaustion of the modified SCB fixed-bed column, desorption experiment was carried out by pumping ethylenediaminetetraacetic acid disodium salt ( $0.005 \text{ mol L}^{-1}$ ) as eluent at the flow rate of  $6.25 \text{ mL min}^{-1}$ . Concentrations of  $\text{Pb}^{2+}$  and  $\text{Cu}^{2+}$  in the eluate at time  $t$  ( $C'_t$ ,  $\text{mg L}^{-1}$ ) were determined. The amount of metal ions desorbed at time  $t$  ( $q'_t$ ,  $\text{mmol g}^{-1}$ ) is calculated by Eq. 2.

$$q'_t = \frac{v \int_{t=0}^{t=t} C'_t dt}{m} \quad (2)$$

## Results and discussion

### Characterization

EDX analysis showed that the nitrogen element content on the unmodified SCB was under detection limit, and it increased to 5.35 % after modification. FTIR spectra of the modified and unmodified SCB are shown in Fig. 1. Peaks at 3450, 1740, 1660, 1652, 1400, 1368  $\text{cm}^{-1}$  are observed in the unmodified SCB spectrum. The peak at 3450  $\text{cm}^{-1}$  is

attributed to the stretching vibration of hydroxyl groups. The peak observed at 1740  $\text{cm}^{-1}$  is due to the carbonyl stretching vibration of ester and carboxyl groups in hemicelluloses. Peaks at 1660 and 1652  $\text{cm}^{-1}$  are corresponding to the carbonyl stretching vibration of amide groups. The peaks at 1400 and 1368  $\text{cm}^{-1}$  are attributed to C–H flexing vibration in hemicelluloses, respectively. One new peak at 1635  $\text{cm}^{-1}$  assigned to the –N–H flexing vibration appeared on the modified SCB, demonstrating that amine groups were introduced onto the SCB surface. The above results showed that TEPA was successfully grafted on the SCB surface. Because there are five amine groups in a TEPA molecule,  $\text{Cu}^{2+}$  can interact with four of the five amine groups and form the  $\text{Cu}^{2+}$ -amine coordination compound (shown in inset of Fig. 1).

### Batch adsorption

Figure 2 shows the adsorption isotherms of  $\text{Cu}^{2+}$  on the unmodified and modified SCB. It was observed that the amount of the adsorbed metal ion increased with an increase in equilibrium concentration and ultimately attained a saturated value. The adsorption data were analyzed by using the Langmuir model, and the calculated  $q_m$  (the maximum amount of  $\text{Cu}^{2+}$  adsorbed) for the unmodified and modified SCB were 0.12 and 0.21  $\text{mmol g}^{-1}$ , respectively. The percentage deviations of the experimental and calculated  $q_m$  for unmodified and modified SCB were 1.6 % and 2.9 %, respectively. The inset in Fig. 2 shows the effects of pH on the  $\text{Cu}^{2+}$  adsorption. It was observed that the optimum pH range for  $\text{Cu}^{2+}$  adsorption was from 4.0 to 6.0. Similar results were reported by Shen et al. (2012). At a low solution pH, the primary and secondary amine groups were easy to protonize to  $-\text{NH}_3^+$  and  $\text{NH}_2^+$ , which would inhibit the coordination of  $\text{Cu}^{2+}$ . At a high solution pH, the protonating ability of amine groups

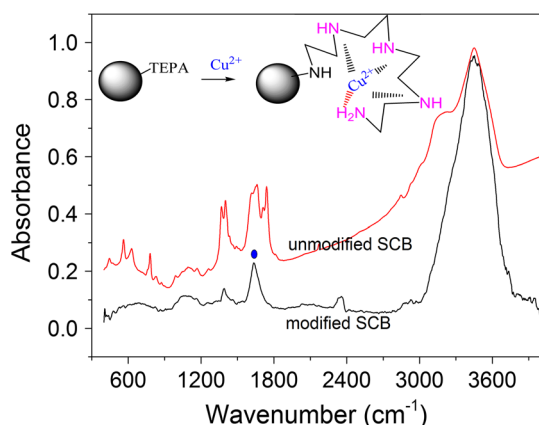


**Fig. 1** FTIR spectra of the modified and unmodified SCB. *Inset* Adsorption mechanism of  $\text{Cu}^{2+}$  on the modified SCB

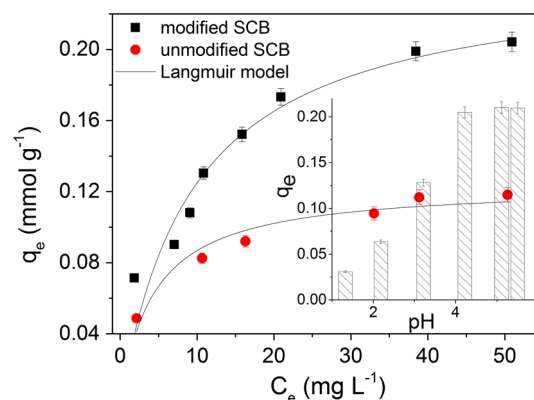


**Fig. 2** Adsorption isotherm of  $\text{Cu}^{2+}$  on the modified and unmodified SCB. *Inset* effects of pH on the adsorption of  $\text{Cu}^{2+}$  on the modified SCB

was weakened and more amine groups could coordinate with  $\text{Cu}^{2+}$ ; this led to an increase of the adsorption capacity of the modified SCB. In order to prevent the precipitation of  $\text{Cu}^{2+}$  and  $\text{Pb}^{2+}$ , a pH of 4.0 was selected for further adsorption experiments.

### Adsorption of $\text{Cu}^{2+}$ and $\text{Pb}^{2+}$ on the modified SCB fixed-bed column in the unitary system

Breakthrough curves of  $\text{Cu}^{2+}$  at different flow rate are present in Fig. 3a. For comparison, blank breakthrough curves of  $\text{Cu}^{2+}$  with no SCB fixed were carried out at the flow rate of  $6.25 \text{ mL min}^{-1}$ . It was observed that the breakthrough curves of  $\text{Cu}^{2+}$  in the fixed-bed column showed an obvious “S” shape. Due to the large amount of active sites (amine groups) on the sorbent surface,  $\text{Cu}^{2+}$  was removed completely from the aqueous solution at the beginning, and the breakthrough time ( $C_t/C_0 = 0.05$ ) at flow rate of  $3.00$  and  $6.25 \text{ mL min}^{-1}$  was 90 and 29 min, respectively. With the occupation of amine groups, part of the metal ions could not be adsorbed and began to flow out, and  $C_t/C_0$  increased sharply to 1.0 till the column

exhausted. The amount of metal ions adsorbed at time  $t$  was calculated and shown in Fig. 3a, and the saturated capacity of the column obtained at flow rate of  $3.00$  and  $6.25 \text{ mL min}^{-1}$  was  $0.22$  and  $0.21 \text{ mmol g}^{-1}$ , respectively, demonstrating that adsorption of  $\text{Cu}^{2+}$  on the modified SCB was a rapid process and it was almost not affected by changes in the flow rate in our investigated range. The adsorption capacity obtained in the dynamic system was similar to that obtained in the batch system. With consideration to the time needed and the adsorption capacities of the modified SCB, a flow rate of  $6.25 \text{ mL min}^{-1}$  was chosen in the following experiment.

Blank and breakthrough curves of  $\text{Pb}^{2+}$  in the unitary system at flow rate of  $6.25 \text{ mL min}^{-1}$  were also conducted and are shown in Fig. 3b. Breakthrough time of the column for  $\text{Pb}^{2+}$  was 7 min. According to the breakthrough curves, the saturated capacity for  $\text{Pb}^{2+}$  was calculated to be  $30.7 \text{ mg g}^{-1}$ .

### Selective adsorption and separation of $\text{Cu}^{2+}$ from $\text{Pb}^{2+}$ by the modified SCB fixed-bed column

Separation of  $\text{Cu}^{2+}$  and  $\text{Pb}^{2+}$  was conducted in the fixed-bed column under dynamic system. Figure 4a shows the breakthrough curves of  $\text{Cu}^{2+}$  and  $\text{Pb}^{2+}$  at  $C_0^{\text{Cu}}/C_0^{\text{Pb}} = 1:1$ . Results showed that breakthrough time for  $\text{Cu}^{2+}$  and  $\text{Pb}^{2+}$  was 30 and 15 min, respectively. The faster breakthrough time of  $\text{Pb}^{2+}$  was due to its lower adsorption affinity to the biosorbent (Sag and Kutsal 2001; Kratochvil and Volesky 1998). It was also observed that  $\text{Cu}^{2+}$  does not overshoot in the whole process, while  $\text{Pb}^{2+}$  overshoots the normal maximum dimensionless value of 1.0 to 1.7 at 30 min. The high overshoot illustrated that  $\text{Pb}^{2+}$  was pushed off by  $\text{Cu}^{2+}$  during the sorption process and substitution of previously adsorbed  $\text{Pb}^{2+}$  occurred with the saturation of the sorbent. Similar results were also reported by Escudero et al. (2013). In order to further clarify the substitution reaction, the amount of metal ions adsorbed onto the column ( $q_t$ ,  $\text{mmol g}^{-1}$ ) as a function of time is depicted in Fig. 4b. The  $q_t$  of  $\text{Cu}^{2+}$  increased continuously until the equilibrium was obtained, while that of  $\text{Pb}^{2+}$  decreased substantially after the maximum adsorption at 25 min. The variation of the values of  $q_t$  shows that the competitive substitution reaction between  $\text{Cu}^{2+}$  and  $\text{Pb}^{2+}$  occurred at a time of 25 min and ended at a time of 150 min. In this process, about  $0.07 \text{ mmol g}^{-1}$  of  $\text{Pb}^{2+}$  was replaced by  $\text{Cu}^{2+}$ . The adsorption schedule of  $\text{Cu}^{2+}$  and  $\text{Pb}^{2+}$  in the modified SCB fixed-bed column is shown in Fig. 5. At the exhaustion of the column, the amount of  $\text{Cu}^{2+}$  adsorbed was  $0.19 \text{ mmol g}^{-1}$ , while that of  $\text{Pb}^{2+}$  was below  $0.001 \text{ mmol g}^{-1}$ . The mole concentration ratio of  $\text{Cu}^{2+}$  and  $\text{Pb}^{2+}$  absorbed in the column was higher than 190:1, suggesting that  $\text{Cu}^{2+}$  was adsorbed selectively from the mixture solution. It had been reported that both  $\text{Cu}^{2+}$  and

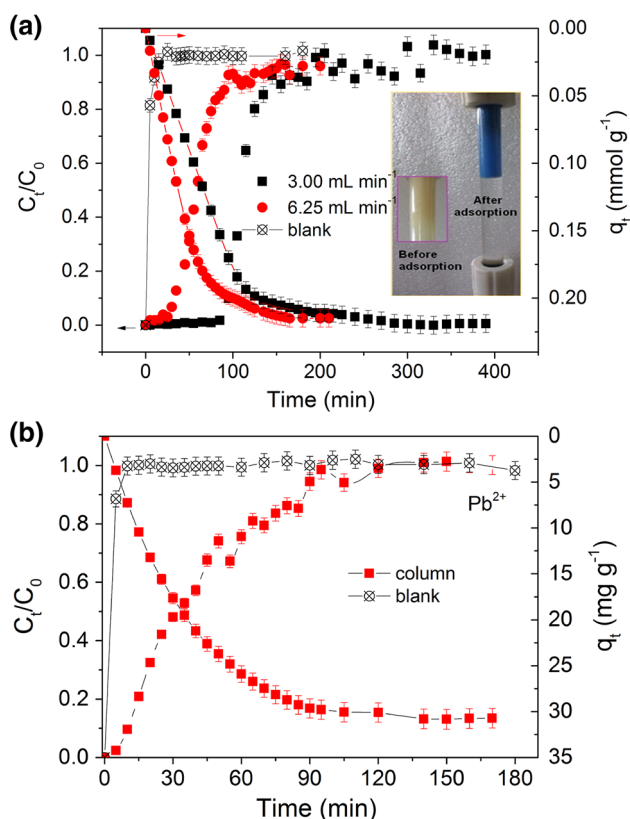


**Fig. 3** Breakthrough curves and dynamic adsorption kinetic of (a)  $\text{Cu}^{2+}$  and (b)  $\text{Pb}^{2+}$  on the fixed-bed column (amount of sorbent =  $0.5 \text{ g}$ , inlet concentration of  $\text{Cu}^{2+} = 20 \text{ mg L}^{-1}$ , flow rate =  $6.25 \text{ mL min}^{-1}$ , pH = 4.0). Inset: photographs of the fixed-bed column before and after  $\text{Cu}^{2+}$  adsorption



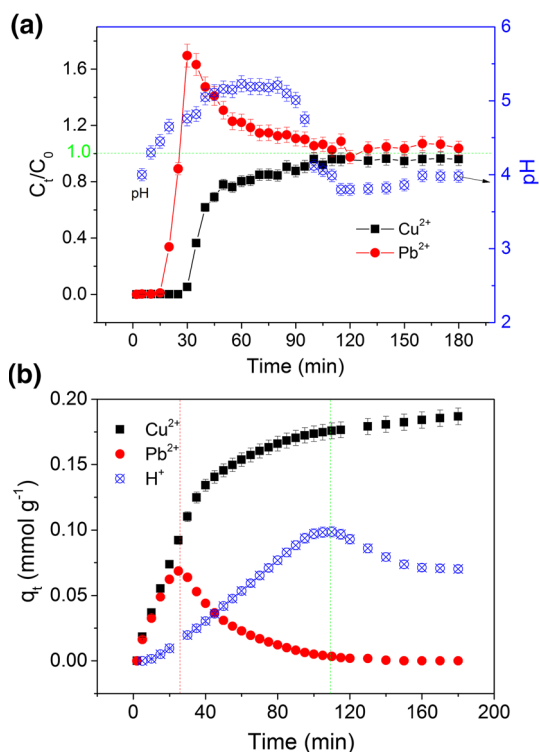


**Fig. 4** (a) Breakthrough curves and (b) amount of  $\text{Cu}^{2+}$ ,  $\text{Pb}^{2+}$  and  $\text{H}^+$  adsorbed on the modified SCB fixed-bed column in the binary system (amount of sorbent = 0.5 g, inlet concentration of  $\text{Cu}^{2+}$  = 20 - mg  $\text{L}^{-1}$ , mole ratio of  $\text{Pb}/\text{Cu}$  = 1:1, flow rate = 6.25 mL  $\text{min}^{-1}$ , pH = 4.0)

$\text{Pb}^{2+}$  could coordinate with amine groups (Kuang et al. 2013; Deng et al. 2013). However, the higher coordination ability of amine groups toward  $\text{Cu}^{2+}$  made it preferentially adsorbed (Deng and Ting 2005). Liu et al. (2010) had reported that for TEPA-modified sorbent which contains five nitrogen atoms in a ligand, 4 N-Cu may be predominating in the coordination. The formation of blue compound in our experiment (inset in Fig. 3) also demonstrated the coordination of  $\text{Cu}^{2+}$  with amine groups.

The variation of solution pH during the sorption process was also determined and is depicted in Fig. 4a. It was observed that the solution pH first increased to a maximum plateau at pH ~ 5.2, and then decreased significantly to pH 3.8 (below the initial pH 4.0) at a time of 115 min. After 160 min, the solution pH approached the initial pH and equilibrium was obtained. Zeta potential of the modified SCB

obtained at pH 2.0, 4.0, 6.0, 8.0, 10.1, 11.0 and 12.1 were 31.1, 24.5, 19.1, 9.6, -4.6, -15.9 and -15.1, respectively, and the point of zero charge was at pH 9.7. At the beginning of the adsorption process, amine groups on the modified SCB would accept proton, which lead to the increase of the solution pH to 5.2. After 60 min, with the protonation of these functional groups, no more sites could accept proton, and the solution pH returned to the initial value of 4.0. The continuous decrease of pH to 3.8 after 110 min may be ascribed to the release of  $\text{H}^+$  from the protonated amine groups. The amount of  $\text{H}^+$  adsorbed during this process is calculated by using Eq. 3 and shown in Fig. 4b.

$$q_t^H = \frac{v \int_{t=0}^{t=t} (C_0^H - C_t^H) dt}{m} \tag{3}$$

The maximum and equilibrium amount of  $\text{H}^+$  adsorbed was 0.1 and 0.07  $\text{mmol g}^{-1}$ , respectively, demonstrating that about 0.03  $\text{mmol g}^{-1}$  of  $\text{H}^+$  on amine groups was replaced. From the time required for  $\text{Pb}^{2+}$  and  $\text{H}^+$  to be substituted, it was concluded that  $\text{Pb}^{2+}$  was replaced by  $\text{Cu}^{2+}$  first and then  $\text{H}^+$  was replaced.

In order to further determine the interference of  $\text{Pb}^{2+}$  on  $\text{Cu}^{2+}$  adsorption, adsorption of  $\text{Cu}^{2+}$  at high values of  $C_0^{\text{Cu}}/C_0^{\text{Pb}}$  (1:10 and 1:100) was studied. Figure 6 shows the effects of  $C_0^{\text{Cu}}/C_0^{\text{Pb}}$  on the breakthrough curves and amount of  $\text{Cu}^{2+}$  adsorbed in the column. Breakthrough time obtained at the molar ratios of 1:1, 1:10 and 1:100 was 30, 30 and 35 min, and the maximum of  $\text{Cu}^{2+}$  adsorbed was 0.19, 0.21 and 0.20  $\text{mmol g}^{-1}$ , respectively. These results demonstrated that the adsorption of  $\text{Cu}^{2+}$  was insignificantly affected by the presence of  $\text{Pb}^{2+}$  in our investigated range.

In order to describe the fixed-bed column behavior and scale it up for industrial applications, the breakthrough curves of  $\text{Cu}^{2+}$  in single ion and binary systems were fitted to the Yoon–Nelson model (Eq. 4).

$$\frac{C_t}{C_0} = \frac{1}{1 + \exp(-k(t - \tau))} \tag{4}$$

where  $k$  is the rate constant ( $\text{min}^{-1}$ ) and  $\tau$  (min) is the time required for reaching 50 % adsorbate breakthrough (min). The fitted results were listed below:

$\text{Cu}^{2+}$  in single ion system

$$\frac{C_t}{C_0} = \frac{1}{1 + \exp(-0.08(t - 59.19))} \quad R^2 = 0.986 \tag{5}$$

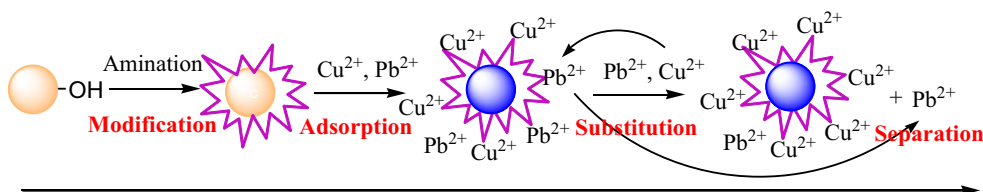


**Fig. 5** Adsorption schedule of  $\text{Cu}^{2+}$  and  $\text{Pb}^{2+}$  on the modified SCB fixed-bed column

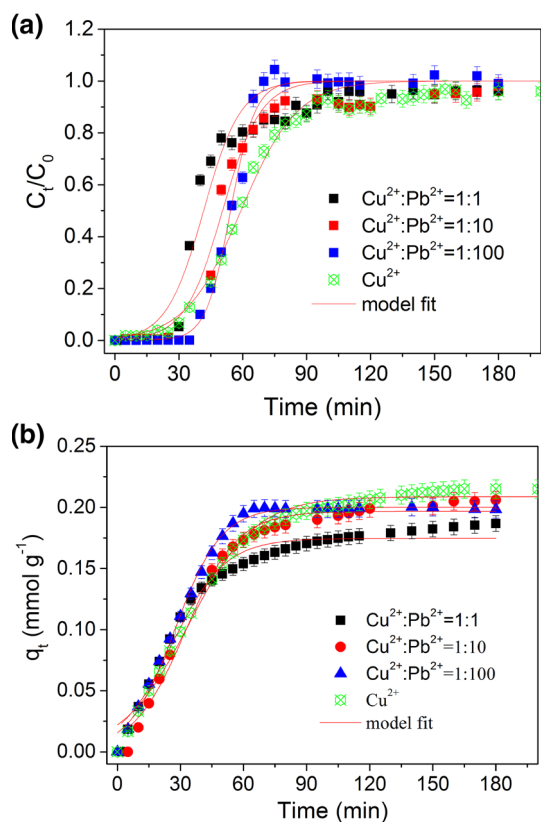


**Fig. 6** Effects of molar concentration on the **a** breakthrough curves and **b** amount of  $\text{Cu}^{2+}$  adsorbed on the modified SCB fixed-bed column in the binary system (amount of sorbent = 0.5 g, inlet concentration of  $\text{Cu}^{2+}$  = 20 mg  $\text{L}^{-1}$ , flow rate = 6.25 mL  $\text{min}^{-1}$ , pH = 4.0)

$\text{Cu}^{2+}$  in binary system

$\text{Cu}^{2+}:\text{Pb}^{2+} = 1:1$

$$\frac{C_t}{C_0} = \frac{1}{1 + \exp(-0.11(t - 41.59))} \quad R^2 = 0.947 \quad (6)$$

$\text{Cu}^{2+}:\text{Pb}^{2+} = 1:10$

$$\frac{C_t}{C_0} = \frac{1}{1 + \exp(-0.11(t - 50.55))} \quad R^2 = 0.974 \quad (7)$$

$\text{Cu}^{2+}:\text{Pb}^{2+} = 1:100$

$$\frac{C_t}{C_0} = \frac{1}{1 + \exp(-0.17(t - 54.32))} \quad R^2 = 0.995 \quad (8)$$

The values of  $R^2$  showed that the Yoon–Nelson model match the curves well.  $\tau$  calculated by the model were very close to the experimental values.

Since all the breakthrough curves matched the Yoon–Nelson model well, the attempt to find the relationship between  $q_t$  and time  $t$  was tried by using a modified Yoon–Nelson model (Eq. 9).

$$q_t = \frac{q_m}{1 + \exp(-k'(t - \tau'))} \quad (9)$$

where  $k'$  is the adsorption constant ( $\text{min}^{-1}$ ),  $\tau'$  (min) is the time required for reaching 50 % of the total adsorption amount (min) and  $q_m$  is the calculated adsorption capacity. Calculated parameters are shown in Eq. (10–13). High values of  $R^2$  showed that the modified Yoon–Nelson model predicted the data well, and the obtained  $q_m$  and  $\tau$  in single and binary system were both very close to experimental values.

$\text{Cu}^{2+}$  in single ion system

$$q_t = \frac{0.21}{1 + \exp(-0.063(t - 33.96))} \quad R^2 = 0.990 \quad (10)$$

$\text{Cu}^{2+}$  in binary system

$\text{Cu}^{2+}:\text{Pb}^{2+} = 1:1$

$$q_t = \frac{0.18}{1 + \exp(-0.079(t - 25.74))} \quad R^2 = 0.975 \quad (11)$$

$\text{Cu}^{2+}:\text{Pb}^{2+} = 1:10$

$$q_t = \frac{0.20}{1 + \exp(-0.080(t - 32.25))} \quad R^2 = 0.987 \quad (12)$$

$\text{Cu}^{2+}:\text{Pb}^{2+} = 1:100$

$$q_t = \frac{0.20}{1 + \exp(-0.091(t - 27.35))} \quad R^2 = 0.995 \quad (13)$$

#### Elution of $\text{Cu}^{2+}$ and $\text{Pb}^{2+}$ from the saturated fixed-bed column

In order to further demonstrate the selectivity of the modified SCB, elution of  $\text{Cu}^{2+}$  and  $\text{Pb}^{2+}$  from the saturated fixed-bed column by using EDTA-2Na (0.005 mol  $\text{L}^{-1}$ ) as the eluent was carried out. The use of EDTA-2Na allows the biosorbent reutilization in a rapid and efficient way. Figure 7a–c depicts the elution curves of the two metal ions from the saturated column obtained at different  $C_0^{\text{Cu}}/C_0^{\text{Pb}}$ . The elution of both the metal ions reached equilibrium after 15 min of desorption. The desorption amount of the two metal ions ( $q_t'$ ) at different  $C_0^{\text{Cu}}/C_0^{\text{Pb}}$  was calculated and shown in Fig. 8. When  $C_0^{\text{Cu}}/C_0^{\text{Pb}}$  varied from 1:1, 1:10 and 1:100,  $q_t'$  of  $\text{Cu}^{2+}$  were 0.16, 0.16 and 0.15 mmol  $\text{g}^{-1}$ , while that of  $\text{Pb}^{2+}$  were 0.0016, 0.0051 and 0.0094 mmol  $\text{g}^{-1}$ , respectively. The desorption efficiencies were higher than 80 % for both of the two metal ions. Desorption of the column resulted in high  $\text{Cu}^{2+}$  concentration eluate. The molar concentration ratio of  $\text{Cu}^{2+}$  and  $\text{Pb}^{2+}$  increased from 1:1, 1:10 and 1:100 to 100:1, 31:1 and 16:1, and the mass percentage of  $\text{Cu}^{2+}$  in the solution increased from 23.6, 3.0 and 0.3 % to 96.87, 90.55 and 83.18 %, respectively. The above results demonstrated that the amine groups-modified fixed-bed column could selectively adsorb  $\text{Cu}^{2+}$  from the mixture

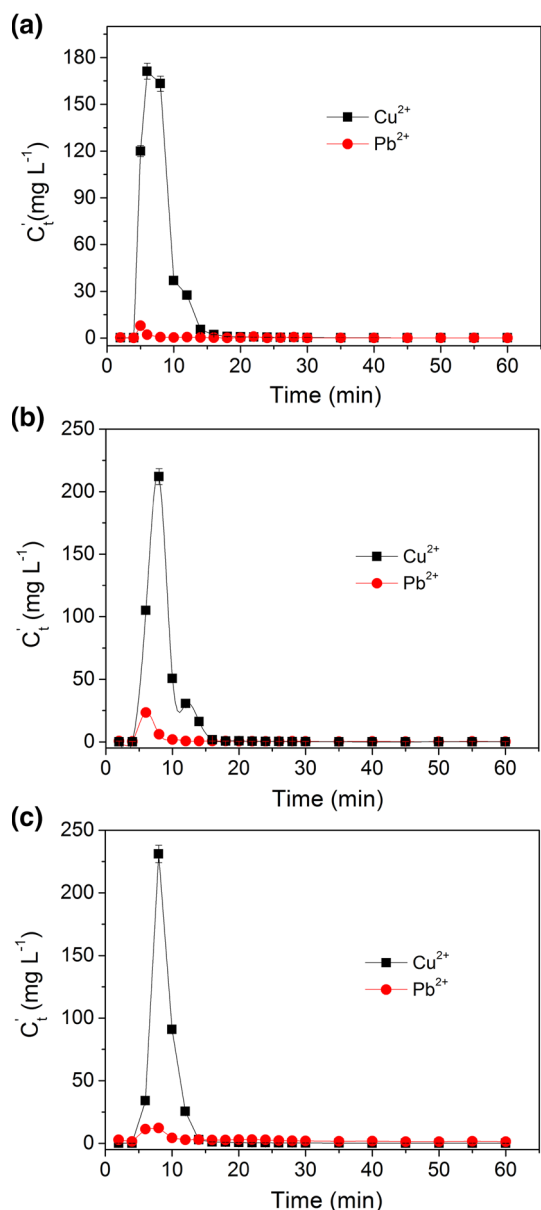


**Fig. 7** Elution curves of the two metal ions from the saturated column obtained in the binary system of  $\text{Cu}^{2+}$  and  $\text{Pb}^{2+}$  at different concentration ratio **a** 1:1, **b** 1:10 and **c** 1:100 (amount of sorbent = 0.5 g, concentration of EDTA-2Na =  $0.005 \text{ mol L}^{-1}$ , flow rate =  $6.25 \text{ mL min}^{-1}$ )

solution, and the content of  $\text{Pb}^{2+}$  was reduced significantly after passing through the column. Even at  $C_0^{\text{Pb}}/C_0^{\text{Cu}} > 100$ ,  $\text{Cu}^{2+}$  could be enriched and separated from the mixture solution through multistage adsorption–desorption cycle.

## Conclusion

TEPA-modified SCB with high adsorption capacity and selectivity toward  $\text{Cu}^{2+}$  was prepared through a simple method. Flow rates had insignificantly effect on the

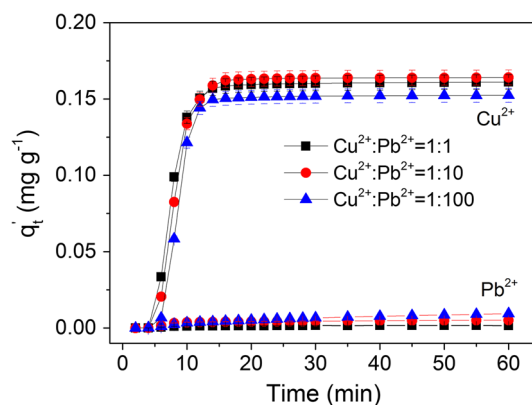


**Fig. 8** Amount of metal ions desorbed from the saturated column obtained in the binary system of  $\text{Cu}^{2+}$  and  $\text{Pb}^{2+}$  at different concentration ratio **a** 1:1, **b** 1:10 and **c** 1:100 (amount of sorbent = 0.5 g, concentration of EDTA-2Na =  $0.005 \text{ mol L}^{-1}$ , flow rate =  $6.25 \text{ mL min}^{-1}$ )

adsorption of  $\text{Cu}^{2+}$  on modified SCB fixed-bed column in our investigated range. The adsorption breakthrough and capacity curves of  $\text{Cu}^{2+}$  in the unitary and binary system both could be predicted well by Yoon–Nelson and modified Yoon–Nelson model, respectively. Dynamic competitive adsorption experiments demonstrated that the modified SCB had higher adsorption affinity toward  $\text{Cu}^{2+}$  than  $\text{Pb}^{2+}$ , and adsorption of  $\text{Cu}^{2+}$  was not affected by the presence of  $\text{Pb}^{2+}$  even at a high concentration ratio of  $C_0^{\text{Cu}}/C_0^{\text{Pb}} = 1:100$ . The amine groups-modified SCB fixed-bed column could be applied in the separation of  $\text{Cu}^{2+}$  and  $\text{Pb}^{2+}$  from aqueous solution.

**Acknowledgments** The work is financially supported by National Natural Science Foundation of China (No. 51574182), the Key Project of Chinese Ministry of Education (No. 213024A) and the program for excellent young scientific and technological innovation team of Hubei Provincial Department of Education, China (No. T201506).

## References

- Bayo J (2012) Kinetic studies for Cd(II) biosorption from treated urban effluents by native grape fruit biomass (*Citrus paradisi L.*): The competitive effect of Pb(II), Cu(II) and Ni(II). *Chem Eng J* 191:278–287
- Deng SB, Ting YP (2005) Characterization of PEI-modified biomass and biosorption of Cu(II), Pb(II) and Ni(II). *Water Res* 39:2167–2177
- Deng YH, Gao ZQ, Liu BZ, Hu XB, Wei ZB, Sun C (2013) Selective removal of lead from aqueous solutions by ethylenediamine modified attapulgite. *Chem Eng J* 223:91–98
- Escudero C, Poch J, Villaescusa I (2013) Modelling of breakthrough curves of single and binary mixtures of Cu(II), Cd(II), Ni(II) and Pb(II) sorption onto grape stalks waste. *Chem Eng J* 217:129–138
- Goyal P, Srivastava S (2009) Characterization of novel Zea mays based biomaterial designed for toxic metals biosorption. *J Hazard Mater* 172:1206–1211



- Hu X, Zhao M, Song G, Huang H (2011) Modification of pineapple peel fiber with succinic anhydride for Cu(II), Cd(II) and Pb(II) removal from aqueous solutions. *Environ Technol* 32:739–746
- Isaac RA, Gil L, Cooperman AN, Hulme K, Eddy B, Ruiz M, Jacobson K, Larson C, Pancorbo OC (1997) Corrosion in drinking water distribution systems: a major contributor of copper and lead to wastewaters and effluents. *Environ Sci Technol* 31:3198–3203
- Kratochvil D, Volesky B (1998) Advances in the biosorption of heavy metals. *Trends Biotechnol* 16:291–300
- Krishnan KA, Sreejalekshmi KG, Baiju RS (2011) Nickel(II) adsorption onto biomass based activated carbon obtained from sugarcane bagasse pith. *Bioresour Technol* 102:10239–10247
- Krishnan KA, Sreejalekshmi KG, Vimexen V, Dev Vinu V (2016) Evaluation of adsorption properties of sulphurised activated carbon for the effective and economically viable removal of Zn(II) from aqueous solutions. *Ecotoxicol Environ Saf* 124:418–425
- Kuang SP, Wang ZZ, Liu J, Wu ZC (2013) Preparation of triethylenetetramine grafted magnetic chitosan for adsorption of Pb(II) ion from aqueous solutions. *J Hazard Mater* 260:210–219
- Liu CK, Bai RB, Hong L, Liu T (2010) Functionalization of adsorbent with different aliphatic polyamines for heavy metal ion removal: characteristics and performance. *J Colloid Interface Sci* 345:454–460
- Madrid JF, Nuesca GM, Abad LV (2014) Amine functionalized radiation-induced grafted water hyacinth fibers for  $Pb^{2+}$ ,  $Cu^{2+}$  and  $Cr^{2+}$  uptake. *Radiat Phys Chem* 97:246–252
- Motsa MM, Mamba BB, Thwala JM, Msagati TAM (2011) Preparation, characterization, and application of polypropylene-clinoptilolite composites for the selective adsorption of lead from aqueous media. *J Colloid Interface Sci* 359:210–219
- Naiya TK, Bhattacharya AK, Mandal S, Das SK (2009) The sorption of lead(II) ions on rice husk ash. *J Hazard Mater* 163:1254–1264
- Nemr AE, El-Sikaily A, Khaled A, Abdelwahab O (2015) Removal of toxic chromium from aqueous solution, wastewater and saline water by marine red alga *Pterocladia capillacea* and its activated carbon. *Arab J Chem* 8:105–117
- Nguyen TAH, Ngo HH, Guo WS, Zhang J, Liang S, Yue QY, Li Q, Nguyen TV (2013) Corrosion in drinking water distribution systems: a major contributor of copper and lead to wastewaters and effluents. *Bioresour Technol* 148:574–585
- Nuić I, Trgo M, Perić J, Medvidovic NV (2013) Analysis of breakthrough curves of Pb and Zn sorption from binary solutions on natural clinoptilolite. *Micropor Mesopor Mater* 167:55–61
- Qaiser S, Saleemi AR, Umar M (2009) Biosorption of lead from aqueous solution by *Ficus religiosa* leaves: Batch and column study. *J Hazard Mater* 166:998–1005
- Rosales E, Ferreira L, Sanromán M, Tavares T, Pazos M (2015) Enhanced selective metal adsorption on optimised agroforestry waste mixtures. *Bioresour Technol* 182:41–49
- Sag Y, Kutsal T (2001) Recent trends in the biosorption of heavy metals: a review. *Biotechnol Bioprocess Eng* 6:376–385
- Shen HY, Pan SD, Zhang Y, Huang XL, Gong HX (2012) A new insight on the adsorption mechanism of amino-functionalized nano- $Fe_3O_4$  magnetic polymers in Cu(II), Cr(VI) co-existing water system. *Chem Eng J* 183:180–191
- Simate GS, Ndlovu S (2015) The removal of heavy metals in a packed bed column using immobilized cassava peel waste biomass. *J Ind Eng Chem* 21:635–643
- Xu D, Tan XL, Chen CL, Wang XK (2008) Adsorption of Pb(II) from aqueous solution to MX-80 bentonite: effect of pH, ionic strength, foreign ions and temperature. *Appl Clay Sci* 41:37–46
- Xu MY, Yin P, Liu XG, Tang QH, Qu RJ, Xu Q (2013) Utilization of rice husks modified by organomultiphosphonic acids as low-cost biosorbents for enhanced adsorption of heavy metal ions. *Bioresour Technol* 149:420–424
- Yu JX, Wang LY, Chi RA, Zhang YF, Xu ZG, Guo J (2015a) Adsorption of  $Pb^{2+}$ ,  $Cd^{2+}$ ,  $Cu^{2+}$  and  $Zn^{2+}$  from aqueous solution by modified sugarcane bagasse. *Res Chem Intermed* 41:1525–1541
- Yu JX, Zhu J, Feng LY, Chi RA (2015b) Simultaneous removal of cationic and anionic dyes by the mixed sorbent of magnetic and non-magnetic modified sugarcane bagasse. *J Colloid Interface Sci* 451:153–160